*MHY7*. The main novel therapeutic approach we provide is the coexistence of an s-ICD together with endovenous left bundle branch pacing to resolve a complex clinical situation. In our patient, when we decided to implant the ICD for secondary sudden cardiac death prevention, no pacing or antitachycardia treatment was expected to be required; hence, to overcome the risks of intravascular lead failure in a young and growing patient, we selected an s-ICD. Nevertheless, when symptomatic atrioventricular block made pacing unavoidable, the left bundle branch pacing option seemed to offer several potential benefits over a single endovenous ICD system: first, the high rate of adverse events with endovascular ICD generator and leads is well known, especially in young patients[2]; in addition, left bundle pacing is an emerging technique to deliver a more physiological pattern of ventricular pacing, generating a narrow QRS complex and promoting atrioventricular and intraventricular synchrony, thus avoiding adverse consequences of right ventricle pacing on left ventricular function and with lower thresholds and higher R detection than His bundle pacing.[3] Finally, a similar paced QRS to the resting QRS allows correct working of the s-ICD, avoiding a failing in electrocardiogram screening and, thus, reducing the chance of inappropriate therapies.

A challenging situation will appear when the s-ICD battery runs out. One option would be to remove the s-ICD system and insert a transvenous defibrillation electrode with a cardiac resynchronization therapy defibrillator device, as long as the girl's size is close to that of the adult. This would allow us to have only 1 generator placed, enhancing the aesthetic result, as well as to dispose of antitachycardia pacing therapy. However, it would mean another element of interference with the tricuspid valve in a young person.

In summary, the combined use of an s-ICD with a left bundle branch pacemaker may be the optimal choice in certain situations, especially in children, in whom deleterious effects of chronic pacing, as well adverse events related to endovenous defibrillator leads, are extremely undesirable.

## CONFLICTS OF INTEREST

M. Álvarez reports personal fees from Boston Scientific and Medtronic, outside the submitted work. The other authors have nothing to disclose.

Francesca Perin,[a,b,*] Manuel Molina-Lerma,[b,c] Juan Jiménez-Jáimez,[b,c] María del Mar Rodríguez-Vázquez del Rey,[a,b] Ángeles Ortega,[d] and Miguel Álvarez[b,c]

[a] *Unidad de Cardiología Pediátrica, Servicio de Pediatría, Hospital Universitario Virgen de las Nieves, Granada, Spain*
[b] *Instituto de Investigación Biosanitaria, ibs.GRANADA, Granada, Spain*
[c] *Unidad de Arritmias, Servicio de Cardiología, Hospital Universitario Virgen de las Nieves, Granada, Spain*
[d] *Unidad de Cardiología Pediátrica, Hospital Universitario Torrecárdenas, Almería, Spain*

* Corresponding author:
*E-mail address:* francescaperin33@gmail.com (F. Perin).

Available online 13 August 2020

## REFERENCES

1. Barriales-Villa R, Centurión-Inda R, Fernández-Fernández X, et al. Severe cardiac conduction disturbances and pacemaker implantation in patients with hypertrophic cardiomyopathy. *Rev Esp Cardiol.* 2010;63:985–988.
2. Janousek J, van Geldorp IE, Krupikova S, et al. Permanent cardiac pacing in children: choosing the optimal pacing site: a multicenter study. *Circulation.* 2013;127:613–623.
3. Li Y, Chen K, Dai Y, et al. Left bundle branch pacing for symptomatic bradycardia: Implant success rate, safety, and pacing characteristics. *Heart Rhythm.* 2019;16:1758–1765.

https://doi.org/10.1016/j.rec.2020.06.021
1885-5857/


## Prognostic value of indexed pulmonary artery diameter assessed by cardiac magnetic resonance imaging in patients with acute heart failure

### *Valor pronóstico del diámetro indexado de la arteria pulmonar mediante resonancia magnética cardiaca en pacientes con insuficiencia cardiaca aguda*

**To the Editor,**

Pulmonary hypertension (PH) is often associated with heart failure (HF) and is a known predictor of morbidity and mortality in patients with acute HF (AHF).[1,2] Invasive measurement of pulmonary pressures is considered the gold standard for the diagnosis of PH but is not routinely performed in patients with HF, and echocardiography-based estimation is the most commonly used noninvasive method. However, PH study by estimating systolic pulmonary arterial pressure (sPAP) on echocardiography is not always feasible, complicating PH assessment in these patients. When sPAP can be calculated, its values correlate poorly with invasive measurements.[3] Consequently, there is increasing interest in the development of other noninvasive imaging indexes to estimate pulmonary arterial pressure. The aim of our study was to evaluate the prognostic value of the indexed pulmonary artery (PA) diameter obtained by cardiac magnetic resonance imaging (cMRI) in patients with AHF.

A total of 1229 patients were admitted to our hospital due to AHF from April 2009 to October 2014. In all, 313 (25%) of these patients were prospectively included if cMRI was performed as part of the etiologic study for HF during hospitalization once they had been stabilized. Bright-blood anatomic sequences were used to measure the indexed PA diameter, and the maximum diameter was calculated for the vessel perpendicular to the longitudinal axis of the common pulmonary artery. Patients were grouped into 4 quartiles according to indexed PA diameter,

**Table 1**
Baseline characteristics

| | |
|---|---|
| *Patients, n* | 313 |
| *Personal history* | |
| Age, y[a] | 70 [60-76] |
| Male sex[a] | 191 (61.0) |
| Hypertension | 240 (76.8) |
| Diabetes mellitus | 149 (47.6) |
| Dyslipidemia | 188 (60.1) |
| Active smoker | 46 (15.9) |
| Former smoker | 100 (34.6) |
| Chronic ischemic heart disease | 124 (42.9) |
| Prior hospitalization for AHF[a] | 143 (45.7) |
| Charlson index[a] | 2 [0-3] |
| *Vital signs* | |
| Heart rate, bpm[a] | 82 [70-95] |
| Systolic blood pressure, mmHg[a] | 135 [115-155] |
| Diastolic blood pressure, mmHg | 78 [70-91] |
| *ECG and echocardiography* | |
| Atrial fibrillation | 89 (28.4) |
| Bundle-branch block | 93 (29.7) |
| LVEF, % | 37 [28-50] |
| LA diameter, mm | 42 [36-47] |
| sPAP, mmHg[b] | 40 [33-51] |
| *cMRI* | |
| LVEF, %[a] | 36 [24-52] |
| LVEDV, mL | 110 [78-140] |
| LVESV, mL | 70 [38-103] |
| RVEF, %[c] | 50 [39-60] |
| RVEDV, mL[c] | 65 [49-88] |
| RVESV, mL[c] | 33 [21-51] |
| *Lab work* | |
| Hemoglobin, g/dL | 12.6 [11.2-14] |
| Sodium, mEq/L | 139 [136-141] |
| eGFR (MDRD), mL/min/1.73 m$^2$[a] | 68 [51-88] |
| NT-proBNP, pg/mL | 3500 [1799-5858] |

AHF, acute heart failure; cMRI, cardiac magnetic resonance imaging; ECG, electrocardiogram; eGFR, estimated glomerular filtration rate; LA, left atrium; LVEDV, left ventricular end-diastolic volume; LVEF, left ventricular ejection fraction; LVESV, left ventricular end-systolic volume; MDRD, Modification of Diet in Renal Disease; NT–proBNP, N-terminal pro-brain natriuretic peptide; RVEDV, right ventricular end-diastolic volume; RVEF, right ventricular ejection fraction; RVESV, right ventricular end-systolic volume; sPAP, systolic pulmonary arterial pressure.
Data are expressed as n (%) or mean [interquartile range].
[a] Variables included in the Cox multivariate models. *P* values: age ($P = .004$), sex ($P = .665$), prior hospitalization for AHF ($P = .865$), Charlson index ($P = .013$), heart rate ($P = .012$), systolic blood pressure ($P = .091$), eGFR ($P = .369$), NT-proBNP ($P < .001$), and LVEF ($P = .100$).
[b] Data available for 179 patients.
[c] Data available for 258 patients.

expressed in mm/m$^2$: Q1 (6.90-12.69), Q2 (12.70-14.59), Q3 (14.60-16.49), and Q4 (16.50-45.40). Echocardiography was also used to calculate left ventricular end-diastolic and end-systolic diameters, left ventricular ejection fraction (LVEF), and sPAP when tricuspid regurgitation was present (n = 179). The correlation between sPAP and indexed PA diameter was assessed by the Spearman correlation coefficient. The primary endpoint of the study was to determine all-cause mortality during follow-up. A multivariate analysis was performed with Cox regression models in which all the variables listed in table 1 were evaluated, with the final model including variables with $P < .10$ and all variables known to be prognostic, regardless of *P* value. The final multivariate models included the following covariables: age, sex, Charlson index, prior hospitalization for AHF, heart rate, systolic blood pressure, estimated glomerular filtration rate, N-terminal pro-brain natriuretic peptide, and LVEF. The discriminatory capacity and the calibration of the model were adequate (Harrell's C-statistic = 0.748; Hosmer-Lemeshow = 0.379). The additional reclassification ability of indexed PA diameter compared with standard multivariate models was assessed by the net reclassification improvement.

The baseline characteristics of the sample are summarized in table 1. The median age was 70 [60-76] years, 61% were men, and 74.4% had LVEF < 50%. During a median follow-up of 2.7 [interquartile range, 1.8-3.7] years, 101 (32.2%) patients died. A stepwise increase was observed in mortality rates (every 10 person-years) from the lower to the upper indexed PA diameter quartiles: 0.49, 1.07, 1.24, and 2.02 for Q1, Q2, Q3, and Q4 respectively ($P < .001$). This increased risk was observed from the start of follow-up and remained constant (figure 1A). In the multivariate analysis, indexed PA diameter was linearly associated with a higher risk of mortality (hazard ratio = 1.07; 95% confidence interval [95%CI], 1.03-1.12; $P < .001$ per 1-mm/m$^2$ increment), as observed in figure 1B. Adding indexed PA diameter to the baseline multivariate models led to significant reclassification (net reclassification improvement = 0.324; 95%CI, 0.050-0.610). The correlation between sPAP and indexed PA diameter was positive and weak (r = 0.16; $P = .048$). Two sensitivity analyses included the same covariables plus sPAP, indexed volumes, and right ventricular ejection fraction, showing that indexed PA diameter continued to behave as a parameter independently associated with a higher risk of death.

At present, there is considerable interest in the search for new noninvasive imaging parameters allowing reliable, reproducible PH calculation in patients with HF. Various cMRI-based noninvasive methods have been recently proposed for PH estimation and have shown prognostic value, among them several right-side parameters, although none of them have been clearly confirmed.[3] This study is the first in the literature to show a strong positive association between indexed PA diameter and the long-term risk of death in a hospitalized population with AHF. It has been postulated that patients with higher indexed PA diameter values are more likely to experience pulmonary vasculature remodeling and, therefore, combined PH. Our data support measuring indexed PA diameter in all patients with HF who have undergone cMRI, in view of its usefulness for risk stratification. However, this is an observational single-center study, and future research is needed to confirm the usefulness and precision of indexed PA diameter, as well as invasive studies to correlate indexed PA diameter with hemodynamic pulmonary parameters and to define the hemodynamic phenotype most closely corresponding to high indexed PA diameter values. Additionally, there are limitations inherent to cMRI, such as scanner availability or tolerance of the decubitus position by AHF patients.

In conclusion, in patients with AHF, increased indexed PA diameter on cMRI is strongly associated with increased long-term mortality risk.

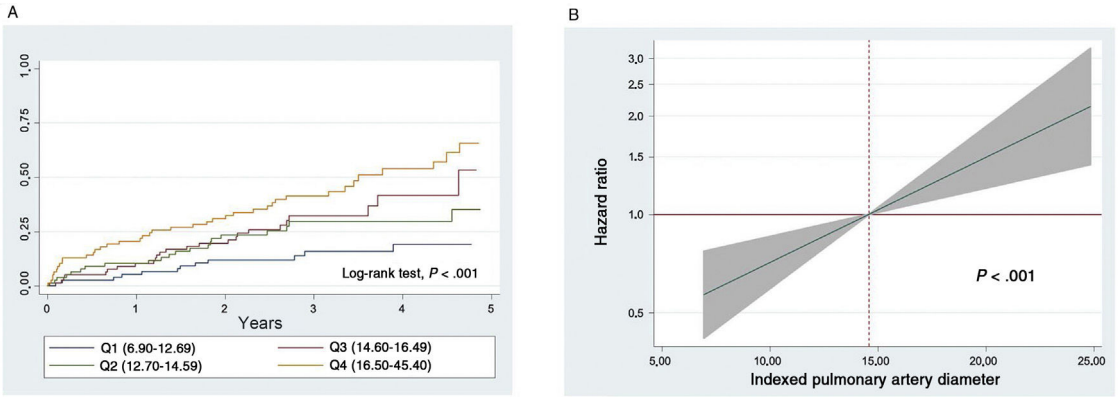


**Figure 1.** A, Kaplan-Meier curves showing all-cause mortality by quartile of indexed pulmonary artery diameter. B, estimated adjusted risk of death according to indexed pulmonary artery diameter.

Julio Núñez,[a] Héctor Merenciano-González,[a] Enrique Santas,[a] María Pilar López-Lereu,[b] José Vicente Monmeneu,[b] and Ernesto Valero[a,*]

[a]*Servicio de Cardiología, Hospital Clínico Universitario, Valencia, Spain*
[b]*Unidad de Resonancia Magnética Cardiaca, ERESA Grupo Médico, Valencia, Spain*

[*] Corresponding author:
*E-mail address:* ernestovaleropicher@gmail.com (E. Valero).

Available online 23 September 2020

## REFERENCES

1. Merlos P, Núñez J, Sanchis J, et al. Echocardiographic estimation of pulmonary arterial systolic pressure in acute heart failure. Prognostic implications. *Eur J Intern Med.* 2013;24:562–567.
2. Santas E, de la Espriella-Juan R, Mollar A, et al. Echocardiographic pulmonary artery pressure estimation and heart failure rehospitalization burden in patients with acute heart failure. *Int J Cardiol.* 2017;241:407–410.
3. Galiè N, Humbert M, Vachiery JL, et al. ESC/ERS Guidelines for the diagnosis and treatment of pulmonary hypertension. *Eur Heart J.* 2016;37:67–119.

https://doi.org/10.1016/j.rec.2020.06.039
1885-5857/


## Valve-in-valve transcatheter aortic valve implantation for bioprosthetic aortic sutureless valve failure: a case series

### *Implante percutáneo de válvula en válvula por fallo de bioprótesis aórtica sin sutura: serie de casos*

**To the Editor,**

In the era of transcatheter aortic valve implantation, sutureless Perceval valves (Livanova, London, United Kingdom) have emerged as a new implantation technique to minimize surgical risk in older patients with multiple comorbidities. This bioprosthesis facilitates a minimally invasive approach, allowing shorter duration of cross-clamping,[1] and prevents patient-prosthesis mismatch because of the absence of a sewing ring, which allows a larger effective orifice area (EOA).[2,3] As a result, sutureless valves have recently been proposed as an ideal solution for elderly patients with a small annulus.

Like other bioprostheses, sutureless valves degenerate; however, stent infolding with distortion (or "stent creep") has been described as a single mechanism of valve failure. It consists of an inward deflection of the stent posts that leads to a reduced EOA, causing high gradients or paravalvular leaks.

Valve-in-valve (ViV) therapy using transcatheter heart valves (THVs) has been shown to be safe and effective in most patients with degenerated prosthetic valves. Nevertheless, little is known about ViV within sutureless valves and only a few cases have been reported.[1,3] We present 5 illustrative cases of sutureless Perceval valve failure occurring at a median time of 3 years after the surgical aortic valve replacement and which were treated between December 2018 and December 2019.

Baseline and procedural characteristics are outlined in table 1. Most of the patients were female and at high risk of aortic valve redo surgery (logistic EuroSCORE = 38.7%, EuroSCORE II = 24.3, and Society of Thoracic Surgeons score = 13.4). The most frequent mechanism of sutureless bioprosthetic failure in our series was stenosis (n = 2), regurgitation (n = 1), and mixed (n = 2). The mechanisms were stent infolding in 2 patients (figure 1), severe aortic regurgitation without evidence of endocarditis on positron emission-computed tomography in 1 patient, and elevated gradients due to calcification and valve degeneration in the other patients. Three of the treated valves were Perceval S (19-21 mm), 1 was Perceval M (21-23 mm), and 1 was Perceval XL (23-25 mm).

Sutureless valves with stent invagination were predilated and postdilated using an Atlas Gold (CR Bard, Murray Hill, New Jersey) balloon catheter in order to make the implantation more predictable. Self-expandable valves (CoreValve Evolut PRO in 1 patient and Symetis ACURATE neo in 1 patient) were used due to their repositionable features and supra-annular design. An Edwards SAPIEN 3 was implanted in the other 3 patients without sutureless valve stent underexpansion with no need for pre- or